# Analysis of Short-Bunch Production with the APS Booster and a Bunch Compressor

Michael Borland, AOD/OAG*

August 8, 2003

## 1 Abstract

There is significant interest among x-ray scientists in short-pulse x-rays. The x-rays from the APS ring, although very bright, are produced by an electron bunch with an rms length of more than 30 ps. Typically, it is only a linear accelerator that can produce a very short bunch. An idea was brought to my attention by Glenn Decker that might allow us to produce a short bunch using the APS booster. This idea involves extracting the beam from the booster at 3 to 4 GeV, while it is still relatively short, then compressing it with a magnetic bunch compressor. In this note, we present a preliminary analysis of this idea, along with the related idea of using a nonequilibrium beam from the APS photoinjector.

## 2 Background

We will begin with an examination of the ideal result we might obtain with linear compression. This will serve to indicate whether the idea is worth exploring through simulation, and also give a rough idea of the required parameters. A diagram of the kind of system we need is shown in Figure 1. This is a standard configuration for bunch compression, consisting of a linear accelerator followed by a magnetic "chicane." The linac applies a chirp to the beam to produce a correlation between arrival time, t, and fractional momentum deviation, $\delta$. Because the time-of-flight in the chicane is momentum-dependent, this chirp results in a modification of the bunch length. The optional post-chicane linac removes the chirp, provided the beam has not been optimally compressed.

Let $(\Delta t_0, \delta_0)$ be the longitudinal phase-space coordinates of a particle at the exit of the booster, where $\Delta t$ is measured relative to the bunch centroid and $\delta$ is the fractional momentum deviation. After transversing the linac, the phase-space coordinates are

$$\Delta t_1 = \Delta t_0 \tag{1}$$

$$\delta_1 = \delta_0 + \frac{V_1}{E}\omega\Delta t_0, \tag{2}$$

where $V_1$ is the rf voltage, $E$ is the beam energy (in volts), and $\omega$ is the angular frequency of the rf. We're assuming here that we traverse the structures at one of the rf zero-crossing points, since there is no reason to accelerate the beam. Consistent with the linear approximation, we're assuming $\sin\omega\Delta t_0 \approx \omega\Delta t_0$.

*Presently on leave of absence at Lyncean Technologies, Inc., Palo Alto, CA

As mentioned, the chicane can be designed to have momentum-dependent time-of-flight, characterized by the $R_{56}$ matrix element, which is defined as $R_{56} = \left(\frac{\partial s}{\partial \delta}\right)_{\delta=0}$, where $s$ is the path length. Hence, at the exit of the chicane, the phase-space coordinates are

$$\begin{aligned} \Delta t_2 = & \quad \Delta t_1 + \delta_1 R_{56}/c & (3)\\ = & \quad \Delta t_0 \left(1 + \tfrac{R_{56} V_1 \omega}{cE}\right) + \delta_0 \tfrac{R_{56}}{c} & (4)\\ \delta_2 = & \quad \delta_1 & (5)\\ = & \quad \delta_0 + \tfrac{V_1}{E}\omega \Delta t_0. & (6) \end{aligned}$$

In the spirit of the linear approximations we're making here, we're ignoring higher-order terms in the chicane transport.

The final rms bunch length is

$$\sigma_{t,2} = \sqrt{\sigma_{t,0}^2 \left(1 + \frac{V_1 R_{56} \omega}{Ec}\right)^2 + \left(\frac{R_{56}\sigma_{\delta,0}}{c}\right)^2}, \tag{7}$$

where we've assumed that the bunch is initially uncorrelated, i.e., $\langle \Delta t_0 \delta_0 \rangle = 0$, which should be accurate for a beam from the booster. We see that the shortest possible bunch is

$$\sigma_{t,2,opt} = \sigma_{\delta,0} \left| \frac{R_{56}}{c} \right|, \tag{8}$$

which is obtained when

$$\frac{V_1}{E} = -\frac{c}{R_{56}\omega} = -\frac{\lambda_{rf}}{2\pi R_{56}}. \tag{9}$$

Note that the condition for the optimum does not depend on the initial properties of the bunch. Typically, we are constrained by $\frac{V_1}{E} << 1$, so we anticipate that we'll need $R_{56} >> \lambda_{rf}/(2\pi) = 0.017$ m. The final rms momentum spread is

$$\sigma_{\delta,2,opt} = \sqrt{(\sigma_{\delta,0})^2 + \left(\frac{c\sigma_{t,0}}{R_{56}}\right)^2}. \tag{10}$$

It turns out that the first term is quite small for beams from the booster at 3 to 4 GeV, so

$$\sigma_{\delta,2,opt} \approx \frac{c\sigma_{t,0}}{|R_{56}|} \tag{11}$$

is a good approximation. We see that $\sigma_{t,2,opt}\sigma_{\delta,2,opt} = \sigma_{t,0}\sigma_{\delta,0}$, as expected from Liouville's theorem. (Alert readers may wonder why this is an exact equality given that we've ignored a term in equation (11). The reason is that there is a small residual chirp on the beam at optimum compression.)

For a given initial momentum spread, obtaining the shortest final bunch requires using small $|R_{56}|$. However, the slope of the required voltage, $V_1\omega$, is inversely proportional to $R_{56}$. Higher voltage and/or higher frequency rf are both undesirable. Higher voltage requires more rf power and more accelerating structures. Higher rf frequency requires smaller structures that are more difficult to build and power. In addition, higher rf frequency makes the rf nonlinearity with time more of an issue.

To be practical, we should use no more than four 3-m-long S-band accelerating structures with a voltage of 50 MV each. These can be driven by a single SLEDed klystron. With a total voltage of 200 MV at $\omega = 2\pi \times 2856$ MHz, we require $|R_{56}| = 0.29$ m for optimum compression at 3.5 GeV.

The equilibrium momentum spread from the booster is $\sigma_{\delta,0} = 0.052\%$. Hence, we can compress to $\sigma_{t,2} = 0.50$ ps.

While this looks promising, there is a potential problem: the required momentum chirp is proportional to $1/R_{56}$. Ignoring for a moment the possibility of a second linac, the larger the momentum chirp, the larger the postcompression momentum spread. For $|R_{56}| = 0.29$ m, the rms momentum spread after the chicane is about 2%. This is larger than the intrinsic linewidth, 1%, from a typical 100-pole undulator, so that the brightness in a 0.1% bandwidth will be reduced considerably compared to a beam with small momentum spread. Using $|R_{56}| = 0.85$ m, which is about as large as seems practical, will decrease the rms momentum spread to about 0.75%. (It also decreases the required rf voltage to about 70 MV, which could be achieved with a single S-band structure powered by a 45-MW klystron.) The downside is that with $|R_{56}| = 0.85$ m, the final rms bunch length is about 1.5 ps. We will compare these two options below and see which offers better performance. We'll refer to the $|R_{56}| = 0.29$ m chicane as the "weak" chicane and the $|R_{56}| = 0.85$ m chicane as the "strong" chicane.

Some might think that adding a second linac after the chicane to remove the momentum spread is a good idea. However, for this to work we cannot optimally compress the bunch. If we do, there is insufficient time-energy correlation remaining to allow removing the chirp. Hence, we'd have to compromise on the peak current. We can see how this might work out by remembering that if the chirp is completely removed, then $\sigma_{t,3}\sigma_{\delta,3} = \sigma_{t,0}\sigma_{\delta,0}$, by Liouville's theorem. Given that the initial bunch length from the booster (see below) is 21 ps, if we elect to make $\sigma_{t,3} = \sigma_{t,0}/10 = 2.1$ ps, then $\sigma_{\delta,3} = 10\sigma_{\delta,0} = 0.5\%$. This is not much smaller than 0.75%, yet the cost is an additional linac after the chicane. This linac must have higher voltage than the first since the bunch to be unchirped is shorter. Hence, it seems we don't gain much from the second linac, and so we've investigated a single-linac system only.

A potentially more profitable option is to add a high-frequency rf system to the booster, to decrease the initial bunch length entering the compressor. A 10-MV system at 2816 MHz ($3456^{th}$ harmonic) would reduce the initial bunch length from 21 ps to 6.7 ps. In the absence of collective effects, this would decrease the postcompression momentum spread threefold (see equation (11)). However, it would not increase the peak current, which depends only on the initial momentum spread and $R_{56}$ (see equation (8)). In a later section of this paper, we explore the feasibility of this approach.

Yet another option is to use a beam from the APS photoinjector, ramped to 3.5 GeV and extracted before it equilibriates. This was previously explored [1] as a possibility for an FEL driver in the water window. It was found that intrabeam scattering and collective effects caused unacceptable degradation of beam properties for this application. In this note, we revisit this scheme to see if it provides a viable alternative to a damped booster beam. One potential downside is that the charge is limited to about 3 nC per pulse.

## 3 Compressor Design

In designing a magnetic compressor, we chose $R_{56}$ to be negative because this is easiest when building a system that has no net bending of the beam (i.e., a chicane). If it is desirable to change the direction of the electron beam, then a positive $R_{56}$ system is best. As is well known, $R_{56} = \int \frac{\eta}{\rho} ds$, where $\eta$ is the dispersion and $\rho$ is the bending radius. Making $R_{56} = -0.85$ m requires either strong bending magnets or weaker bending magnets separated by long drift spaces. To make the chicane as short as possible, we chose a bending field of 1.8 T for both the strong and weak chicanes, giving $\rho \approx 6.5$ m. The system we matched starts with two quadrupoles, followed by the

four dipoles of the chicane, followed by two more quadrupoles. It has mirror symmetry about its midpoint.

We used `elegant`[2] to match the system to the desired $R_{56}$ values. We used the two quadrupoles (outside the dispersion region) to match the beta functions to reasonable values assuming a periodic system. This is just a convenience and can be easily changed once the location of the chicane is made definite. Figure 2 shows the resulting lattice functions for the strong chicane. (The weak chicane is very similar.) For the strong chicane, the bending magnets have angle 0.31 rad and arc length 2.07 m, with an overall length of 19.2 m. For the weak chicane, the bending magnets have angle 0.27 rad and arc length 1.78 m, with an overall length of 14.0 m. About 4 m of the total length in both cases is from the matching section before and after the chicane.

One possibility to shorten the system is to make use of the dispersion from the booster lattice, since this is nonzero in the low-emittance lattice. This could allow us to obtain the desired $R_{56}$ with a shorter system, since we wouldn't need as much space to create dispersion. Putting quadrupoles inside the chicane to increase the dispersion in the two central bends is problematical as it tends to make the system longer and make large beta function variations.

# 4 Initial Tracking Studies

Next, `elegant` was used to track a Gaussian beam with some idealized booster beam properties. In particular, we assumed a booster rf voltage of 8.5 MV, which is the limit of present operations, although the system should be capable of 11 MV [3, 4]. We also used the "92 nm" low-emittance lattice [5] at 3.5 GeV. This gives $\sigma_{t,0} = 21$ ps. We also used the equilibrium emittance of 23 nm with 10% coupling, giving $\epsilon_x = 21$ nm and $\epsilon_y = 2$ nm. A charge of 2 nC per bunch was assumed initially.

The lattice for tracking consisted of four zero-length RFCA rf cavity elements (representing the accelerating structures), with longitudinal wakes. (Using zero-length elements is simply a convenience in that it avoids having to deal with nonessential transverse matching issues.) The RFCAs were phased at the zero crossing to give the proper chirp for compression. `elegant` was then allowed to vary the voltage on the cavities in order to minimize the bunch length. Anticipating that the compression would be nonlinear and that the bunch might therefore have long tails, we used a percentile-based measure of the bunch length, namely, $t_{60\%} - t_{40\%}$, which is the width of the central 20% of the time distribution. This helps `elegant` to find a solution with a high current spike, though maybe not a short rms bunch length.

Figure 3 shows longitudinal phase-space distributions for the strong chicane for two cases: a (fictitious) linear system without wakefields and the system with nonlinearities and wakefields. The difference between these is largely due to the rf curvature effect, which in turn results from the rather long bunch coming from the booster. Figure 4 shows a comparable result for the weak chicane. Again, rf curvature is the dominant nonlinear effect, but second-order effects in the chicane are now more evident, due to the larger momentum offsets.

The rms bunch length is 1.79 ps for the strong chicane and 1.60 ps for the weak chicane. While the former is about 23% larger than the linear model predicts, the latter is more than three times larger. Nonlinearities play a much larger role in the weak chicane because of the larger momentum chirp. Of course, rms bunch length is potentially misleading in the presence of long tails. In fact, for the strong chicane the FWHM bunch length is 3.36 ps, about 7% worse that the linear model predicts. For the weak chicane the FWHM is 1.50 ps, about 30% worse than the linear model predicts. Hence, we still have reason to expect significantly higher peak currents in the small chicane system. For the assumed 2-nC booster bunch, the predicted peak current is 515 A for the

strong chicane and 1241 A for the weak chicane. Figures 5 and 6 show histograms of the time distributions.

We are now in a position to compare the peak brightness obtainable for these two options. This was done assuming a U27 undulator, which has a period of 2.7 cm, 86 effective periods, and $K \leq 2.18$. The current specified for the computation was $I_{50}$, defined as the average current in the central 50% of the bunch. More specifically, $I_{50} = Q/(2\Delta t_{50})$, where $\Delta t_{50}$ is the duration of the central 50% of the beam. For the strong chicane, $I_{50} = 478$ A, while for the weak chicane we get $I_{50} = 1083$ A. Figure 7 shows the peak brightness for the two systems, computed with `sddsbrightness` [6]. Perhaps surprisingly, we see that the strong chicane provides higher peak brightness. This results from the smaller momentum spread and from the comparative lack of nonlinearity in the strong chicane system. Put differently, in the weak chicane we pay a cost in brightness due to larger momentum spread, but due to nonlinearities we don't get the full benefit expected in terms of peak current. The strong chicane system has other advantages. It requires only one 3-m linac structure and no SLED cavity. As a result, in spite of having a longer chicane, the strong chicane system is shorter overall by 3 m. Also, because of the lower peak currents, we expected the strong chicane system to be less affected by coherent synchrotron radiation. In what follows, then, we consider the strong chicane system only.

# 5 CSR and ISR

Two effects in the compression system that might affect these results are coherent synchrotron radiation (CSR) and incoherent synchrotron radiation (ISR). The CSR formation length, $(24\rho^2 c\sigma_t)^{\frac{1}{3}}$, for a 21-ps rms bunch length in the chicane dipole is 1.9 m, slightly shorter than the dipole. However, for a 1-ps rms bunch length, the formation length is 0.69 m, which is less than a of third the dipole length. So one expects that CSR will be generated and will interact with the beam. The full chamber gap required to completely shield CSR from the 1-ps bunch is [7] $0.2(c^2\sigma_t^2\rho)^{\frac{1}{3}}$, or 1.7 mm. This is impractically small, so use of unshielded CSR computations is indicated since we expect most of the CSR effects to happen where the bunch is short.

The CSR simulations used `elegant`'s existing transient computation of unshielded CSR in dipoles and drift spaces downstream of dipoles, based on a 1-dimensional line-charge model [8, 9]. (A discussion of an earlier form of `elegant`'s algorithm is available in [10].) ISR was simulated by assuming the quantum excitation can be characterized by random scattering using appropriately scaled Gaussian distributions, which is also an existing capability of `elegant`. Dipoles were simulated in 100 pieces while drifts were simulated with a step-size of 0.01 m (which is small compared to the minimum formation length).

These tracking simulations used 1 million particles with quiet-start $4\sigma$ Gaussian distributions in all six phase-space coordinates. One thousand bins were used for the CSR computations, which is seen to reproduce the final distribution with little noise. As a result, no smoothing was employed (a conservative choice). Figure 8 shows final beam properties as a function of the bunch charge. We see that CSR has an effect on the beam properties, but it is fairly modest. In addition, at zero charge the horizontal beam emittance is little changed from the 21 nm input value, indicating that ISR is not an important effect even though the dipoles are quite strong.

# 6 Booster Effects

Next, we looked at effects in the booster that might change the extracted beam properties. In this section, we consider the case where we use a damped booster beam. Transient beams are discussed

in a later section. Of concern in both cases are collective effects like intrabeam scattering (IBS) and interaction with the booster vacuum chamber and rf cavities (impedance). We used the "92 nm" low emittance lattice [5] for all calculations.

### 6.1 Intrabeam Scattering

We looked at IBS with the program `ibsEmittance` [6]. For a 10-nC bunch at 3.5 GeV, the IBS growth rate is about 0.004 times the radiation damping rate for both the longitudinal and horizontal planes. Hence, IBS effects are negligible and the equilibrium emittances given by `ibsEmittance` are very close to the nominal values.

The longest radiation damping time is 22 ms (for the horizontal plane). Hence, the beam would need to be stored in the booster for about 50 ms to allow the emittance to damp to within 1% of the equilibrium value.

### 6.2 Impedance Effects

Accurate simulation of impedance effects requires an impedance model, which is not available for the booster. For expediency, I've assumed that the broad-band impedance satisfies $|Z/n| = 0.5\Omega$. This is about equal to the value for the APS storage ring [4], which has far more more "features" in its vacuum chamber than the booster. Hence, we are probably overestimating the booster impedance. In using the broad-band impedance, we are implicitly assuming that all chamber and higher-order-mode resonances are far from revolution harmonics or else strongly detuned. The Boussard criterion

$$q < \frac{(2\pi)^{\frac{3}{2}}\,\alpha(E/e)\sigma_t\sigma_\delta^2}{|Z/n|} \tag{12}$$

can be applied to estimate the longitudinal microwave instability threshold, where $E/e$ is the beam energy in $V$ and $\alpha$ is the momentum compaction factor. The result is 4.5 nC.

To go further, we need an impedance model that will allow us to track beam in `elegant`. A standard model for the broad-band impedance is a $Q = 1$ resonator with the resonant frequency set to the cutoff frequency of the vacuum pipe. For a round pipe, the cutoff frequency is $f_{co} = 2.405c/(2\pi R)$, where $R$ is the radius of the pipe. The booster vacuum pipe is elliptical, so we take $R$ equal to the semi-minor axis, 0.0185 m. For $\omega << \omega_{res}$, the $Q = 1$ resonator impedance is inductive: $Z \approx iR_s\omega/\omega_{res}$, where $R_s$ is the shunt impedance. Expressing $R_s$ in terms of $|Z/n|$ gives $R_s = 2.405\,|Z/n|\,L/(2\pi R)$, where $L$ is the circumference.

To get a starting point for tracking, we used the program `haissinski`[6] to compute the equilibrium density distributions for 1 to 10 nC. The output of `haissinski` was used with `sddssampledist` to generate a set of macroparticles for the distorted distribution for each charge level. These distributions were then tracked for $40,000$ turns (a little over two damping times) using `elegant`, including quantum excitation, radiation damping, and the broad-band impedance. The broad-band impedance was simulated using an `RFMODE` element in single-turn mode. Tracking used the chromatic matrix method with chromatic effects up to third order.

The results of the tracking are shown in Figure 9. We see that the beam properties are fairly insensitive to the charge, much less so than would be naively expected from the Boussard criterion (which predicted instability at 4.5 nC) and the Haissinski equation (which predicted a 25-ps rms bunch length at 10 nC). This is not surprising, however, when one realizes that $1/\sigma_t$ is greater than the cutoff frequency. Hence, the impedance doesn't look like a pure inductor to the beam, contrary to what we assumed in using the Boussard criterion and the Haissinski equation.

The next step is to track the output of the booster through the compressor. For this step, we optimized the compressor for each booster beam, then tracked with CSR and ISR. The results are shown in Figure 10. The first panel shows the peak current, which apparently could be increased further by using more charge. It also shows $I_{50}$, which tracks the peak current quite well. The second panel shows the rms momentum spread, which increases only very slightly from 1 nC to 10 nC. The third panel shows various measures of the bunch length, namely $\Delta t_{50}$ and the FWHM. Again, these are fairly constant, as are the emittances, shown in the last panel.

We used `sddsbrightness` to compute the peak brightness for the compressed beams, assuming a U27 undulator (the properties of which are listed above). The results are shown in Figure 11. For comparison, we also show the peak brightness of the APS ring for a typical 5-mA bunch. One can see that the peak brightness of the compressed booster beam is more than two orders of magnitude *less* than that of the APS. This is partly due to the lower beam energy but it's mostly due to the large emittance of the booster, even at 3.5 GeV. Of course, peak brightness may not be the most important measure of performance. The higher repetition rate and greater length of the APS beam pulses may make their peak brightness hard to utilize.

### 6.3 Use of Higher Harmonic Cavity in the Booster

As mentioned above, one possibility for improving these results is to use a higher harmonic cavity in the booster. Ignoring collective effects, this will decrease the initial longitudinal emittance and result in smaller momentum spread after compression to the same bunch length.

To explore this, we first repeat the above booster simulations with a higher harmonic cavity added. We used a cavity at the $3456^{th}$ harmonic with a voltage of 10 MV. The same broad-band impedance as before was also assumed. As before, beam was tracked with various charge levels for 40,000 turns. Figure 12 displays the results, which show a very surprising feature: the horizontal emittance exhibits a large increase starting at about 4 nC, even though the energy spread and bunch length are little changed. This is certainly related to the fact that there is dispersion at the location of the impedance element (as there is throughout the booster in the low-emittance lattice). The synchrotron tune, $\nu_s$, is close to 0.1 while the horizontal tune is 13.75. Perhaps $2\nu_s \approx 0.2$ is close enough to the horizontal fractional tune to cause a quadrupole instability in the horizontal plane.

Figure 13 shows the results of compressing the beam obtained with the higher-harmonic cavity. The peak current rolls off somewhat due to the increased emittance (which couples into the longitudinal plane in second order), so that the peak current is slightly worse that was obtained without the higher harmonic cavity. The momentum spread is, of course, much less than in the previous case, which was what we expected to achieve. Unfortunately, due to the emittance blow-up, the peak brightness (Figure 14), is not improved except for the low-charge regime.

More study of this case is indicated, in light of the instability. It may be that another choice of cavity properties would yield better results.

## 7 Use of Undamped Photoinjector Beam

In this section, we explore the option of using a beam from the APS photoinjector. In this scheme, instead of allowing the beam to come to equilibrium, we would ramp to 3.5 GeV and extract immediately. The hope is that we can preserve the longitudinal brightness of the photoinjector beam, and hence compress to shorter bunch lengths after extraction. In addition, we would hope to preserve the high transverse brightness of the photoinjector beam. The beam quality reported in the previous simulations of photoinjector beam in the booster [1] seems promising. However,

that work was undertaken before some recent developments, namely, recognition of the importance of the detailed longitudinal distribution and its interplay with CSR. In the prior work, we started with an idealized uniformly distributed beam with the expected properties of the photoinjector beam. In the present study, we used a simulated photoinjector beam from a 1-nC PARMELA run [11], accelerated to 450 MeV without compression.

In [1], we used a heavily modified low-emittance booster lattice, which would involve new magnets. While that is of course still an option (albeit an expensive one), in the present study we used the "92 nm" low emittance lattice. Previously, we included ISR, IBS, and impedance effects, but not CSR. However, the injected beam has an rms duration of several picoseconds. The CSR formation length in the booster dipole ($\rho = 33.3$ m) is 2 m for $\sigma_t = 1$ ps. Since the dipole length is 1.54 m and the required chamber gap for complete shielding a mere 2.9 mm, ignoring CSR is dubious. Since the dipoles are quite close together compared to their length, we've used `elegant`'s steady-state unshielded CSR computation.

Unfortunately, these simulations indicate that the desirable properties of the photoinjector beam, namely, its high longitudinal and transverse brightness, are spoiled by CSR effects in the booster in the first five or ten turns. As Figure 15 shows, the rms momentum spread and bunch length are each increased by more than an order of magnitude from the starting values. As a result, this option is not worth pursuing unless we are willing to contemplate attempting to partially shield the CSR.

In passing, we note that this prediction can be tested in experiments at APS, since there was recent success in accelerating photoinjector beam in the booster [3]. Our prediction is not inconsistent with these results, since we do not predict beam loss, only severe reduction of the brightness. Note that a meaningful test would require stable injection timing, something that has yet to be achieved with the photoinjector and booster.

## 8 Jitter Effects

In addition to collective effects, jitter in the booster beam must be considered. Of concern are jitter in the phase, energy, bunch length, and charge. We've explored these issues for the case without the higher-harmonic cavity and using the strong chicane.

1. Extraction phase can vary due to

   (a) Variation in relative rf phase between the booster and compressor linac rf system.

   (b) Variation in the synchronous phase due to variation in booster rf voltage.

   (c) Variation in the synchronous phase due to variation in beam charge (which varies the energy loss per turn through the impedance).

   Whatever the source, variation in extraction phase changes the arrival time of the beam in the linac, introducing post-chicane beam energy jitter. Due to nonlinearity, it will also affect the compression.

   Because the total energy loss per turn, $U_1$, is small compared to the rf voltage, $V$, the synchronous phase is approximately $\phi_s = \pi - U_1/V$. The energy loss per turn is $U_1 = U_0 + K * q$, where $U_0 = 0.399$ MeV is the energy loss per turn due to synchrotron radiation and $K$ is a constant proportional to the chamber impedance. Letting $\Delta q$ represent the charge "error" and $\Delta V$ the voltage error, we have

$$\Delta\phi_s = \frac{K\Delta q}{V} + \frac{U_1}{V}\frac{\Delta V}{V}. \tag{13}$$

The arrival time variation is

$$\Delta t_a = \frac{K\Delta q}{V\omega_{rf}} + \frac{U_1}{V\omega_{rf}}\frac{\Delta V}{V}, \tag{14}$$

where $\omega_{rf}$ is the booster rf angular frequency. Tracking with `elegant` for the model broad-band impedance discussed above gives $K = 0.00332$ MeV/nC. Hence,

$$\Delta t_a(ps) \approx 0.176\Delta q(nC) + 20.7\frac{\Delta V}{V}, \tag{15}$$

where I've used $U_1 \approx U_0$, $V \approx 8.5$ MV, and $f_{rf} = 352$ MHz.

2. Beam energy can jitter due to cycle-to-cycle variation in the dipole power supply. The fractional beam energy jitter is simply the fractional power supply jitter.

3. Bunch length can jitter due to

   (a) Variation in rf voltage.

   (b) Variation in beam energy.

   (c) Variation in synchronous phase due to variation in beam charge.

   (d) Variation in collective effects due to variation in beam charge.

   The bunch length is

$$\sigma_t = \sigma_{t0}\sqrt{(1+\Delta E/E_0)(1-\Delta V/V_0)\frac{\cos\phi_{s0}}{\cos(\phi_{s0}+\Delta\phi_s)}}. \tag{16}$$

   Using $\phi_s = \pi - U_1/V$ with $U_1/V << \pi$, we see that the cosine terms are quadratic in small quantities and hence negligible. Therefore,

$$\Delta\sigma_t \approx \frac{\sigma_{t0}}{2}\left(\Delta E/E_0 - \Delta V/V_0\right). \tag{17}$$

4. Charge can jitter due to variation in charge from the injector linac and variable capture efficiency in the PAR and booster.

We performed jitter simulations with `elegant` using Gaussian booster beams with a charge of 10 nC. The rms jitter levels were chosen based on estimates of present performance of APS systems:

- Booster energy [4]: 0.015%
- Booster rf voltage: 0.1%.
- Booster output charge: 10%.
- Relative rf phase: 1 degree S-band.
- Linac rf voltage: 0.1%.

The first three levels were used with equations (15) and (17) to determine the initial conditions for 250 random cases of booster beam. For expediency, the 10-nC booster beam from the long-term tracking was used. The length was increased multiplicatively using the factor indicated in equation (17). (Ideally, we would track in the booster for 40,000 turns for each case, to get the effect of charge jitter on equilibrium bunch length. This should be done in the future if evaluation of the

initial results are considered promising.) For each of these beams, the second two jitter levels were used to obtain a linac phase offset and voltage error. Tracking through the compressor ignored CSR, again for reasons of speed, and because CSR is not a major effect, particularly on the peak current.

Figure 16 shows histograms of several important quantities over 250 jitter trials. Statistics on the quantities are in the plot labels. Overall, the performance is good. The jitter in the arrival time is comparable to the bunch length, indicating the experiments will have to use a beam-based trigger method. The rms jitter in the momentum centroid (about 0.04%) is small compared to the momentum spread (about 0.75%). About 80% of both the jitter in the arrival time and momentum centroid is due to booster-to-linac phase jitter. Since the momentum centroid jitter is still modest, we can increase the tolerance on booster-to-linac phase from 1° S-band to perhaps five or ten times that.

# 9 Conclusions

We have explored the possibility of producing short electron bunches with an energy of 3.5 GeV using the APS booster and a downstream magnetic compression system. The required system is about 16 m long (excluding matching sections) and requires one S-band linac structure. We find that rms bunch lengths of 1 to 2 ps are possible, giving peak currents of up to 2.5 kA. We explored jitter sensitivity and found that the system is likely to be sufficiently stable for achievable tolerance levels. X-ray experimenters will have to trigger data collection from the beam pulse, however, because of the fairly large beam timing jitter.

Two potential ways to obtain better results are to extract the beam at lower energy and use a higher-harmonic cavity in the booster. We explored the latter and found that it is not workable, due to increased collective effects in the booster. We also explored the option of using a high-brightness photoinjector beam, but found that CSR effects made this fruitless. We suggest an experimental test of this prediction be made.

Some of these conclusions are dependent on the impedance model used for the booster, which is admittedly not precise but probably not far off. Experimental measurements should be undertaken to ascertain how bunch length depends on charge, in order to benchmark our predictions.

Finally, we found that the peak brightness achievable with this scheme is not impressive, being more than two orders of magnitude less than that of the APS storage ring. It falls to the judgment of the experimenters to decide if this scheme provides a useful beam. If peak brightness is less important than bunch length, then the weak-chicane option should be explored more fully.

# 10 Acknowledgements

The author wishes to thank Glenn Decker for bringing this concept to my attention, for pointing out the need to operate at 3 to 4 GeV in order to start with a short bunch, and for reviewing this paper. Glenn informs me that the idea originated with Steve Milton. I also appreciate helpful discussions of most of the issues with Louis Emery, as well as his thorough review of the text. Finally, I appreciate Nick Sereno's comments, which among other things reminded me of the photoinjector option.

## References


[1] M. Borland, L. Emery, "Analysis of a Scheme for a SASE FEL Demonstration in the 2-4 nm Range," Proceedings of the $17^{th}$ Advanced Beam Dynamics Workshop on Future Light Sources, Argonne, IL, ANL-00/8, wg 3-18, 2000.

[2] M. Borland, "elegant: A Flexible SDDS-Compliant Code for Accelerator Simulation," Advanced Photon Source LS-287, September 2000.

[3] N. Sereno, private communication.

[4] L. Emery, private communication.

[5] N. Sereno *et al.*, "Advanced Photon Source Booster Synchrotron Low-Emittance Lattice Commissioning Results," Proceedings of PAC 2003, to be published.

[6] M. Borland *et al.*, "SDDS-Based Software Tools for Accelerator Design," Proceedings of PAC 2003, to be published.

[7] M. Borland, "Coherent Synchrotron Radiation and Microbunching in Bunch Compressors," Proc. 2002 Linac Conference, Gyeongju, Korea, August 19-23, 2002, pp 11-15, 2003.

[8] E. Saldin *et al.*, NIM A **398**, 373 (1997).

[9] G. Stupakov and P. Emma, "CSR Wake for a Short Magnet in the Ultra-Relativistic Limit," SLAC-PUB-9242, May 2002.

[10] M. Borland, "Simple method for particle tracking with coherent synchrotron radiation," Phys. Rev. ST Accel. Beams **4**, 074201 (2001).

[11] J. Lewellen, private communication.

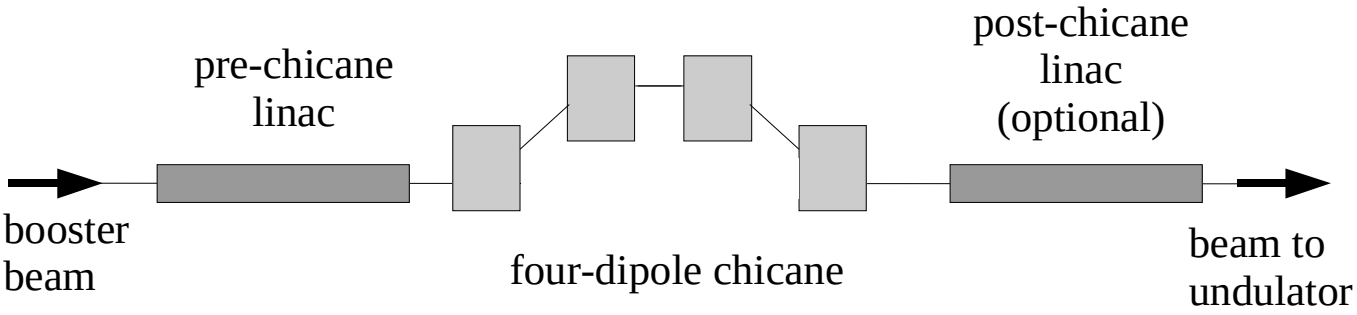


Figure 1: Diagram of a magnetic bunch compression system.

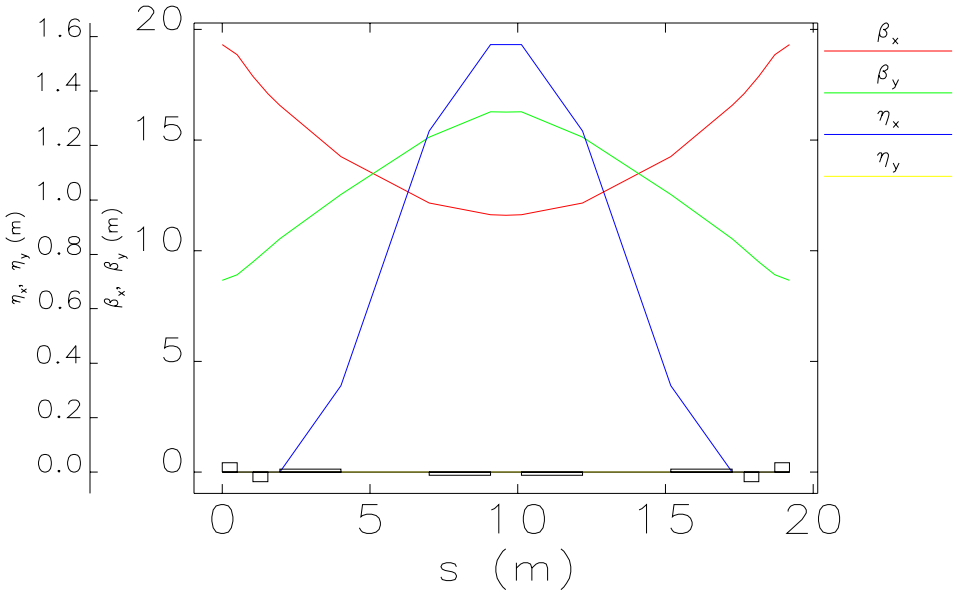


Figure 2: Twiss parameters for the model compressor chicane.

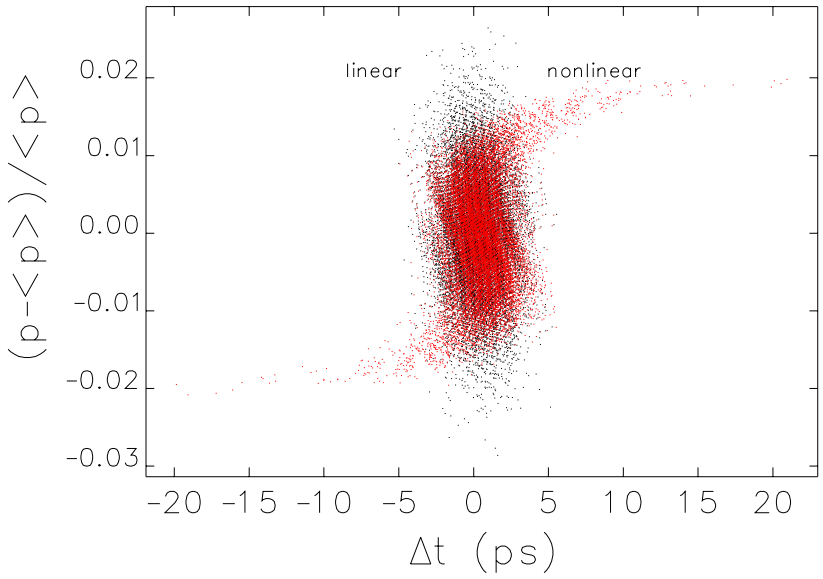


Figure 3: Longitudinal phase space at the exit of the compressor for linear and nonlinear models, for the strong chicane. The symmetric distortion from the nonlinear model indicates that rf nonlinearities are dominant.

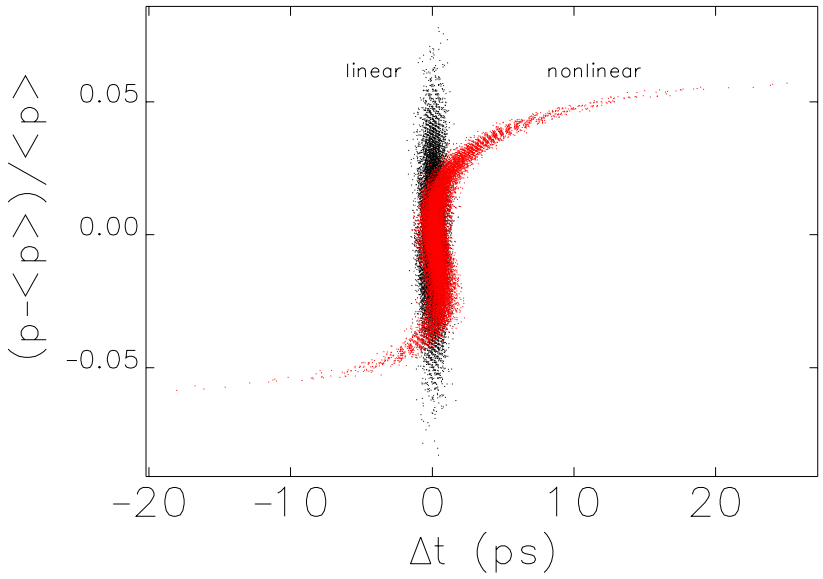


Figure 4: Longitudinal phase space at the exit of the compressor for linear and nonlinear models, for the weak chicane. The slightly asymmetric distortion from the nonlinear model indicates that rf nonlinearities are dominant, but that transport nonlinearities are not negligible.

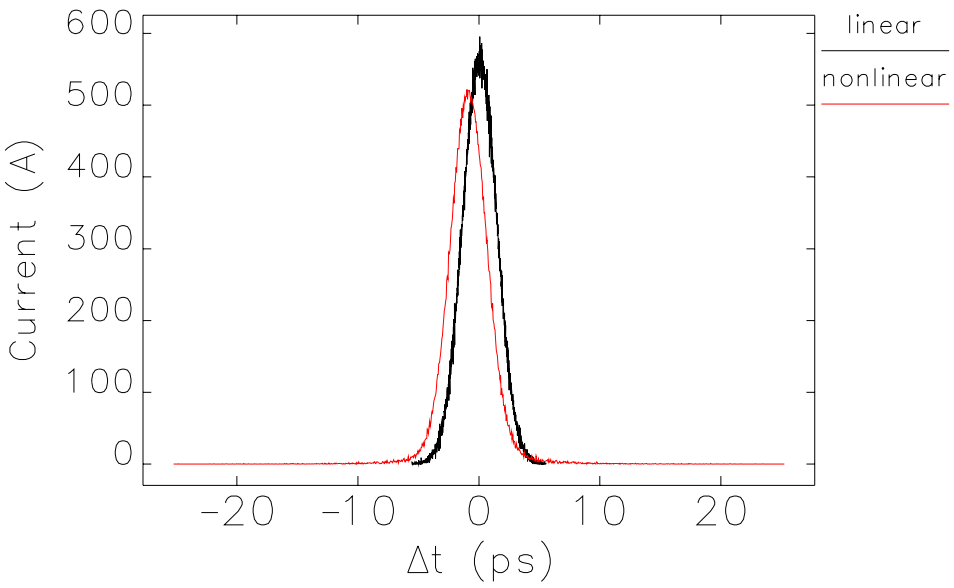


Figure 5: Current histograms at the end of the compressor for 2-nC beam for linear and nonlinear models, for the strong chicane.

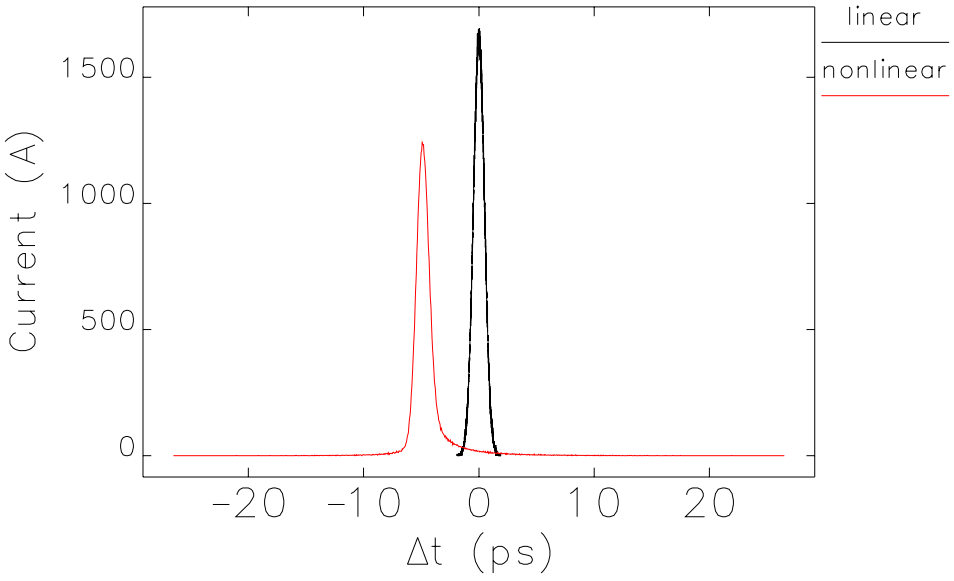


Figure 6: Current histograms at the end of the compressor for 2-nC beam for linear and nonlinear models, for the weak chicane.

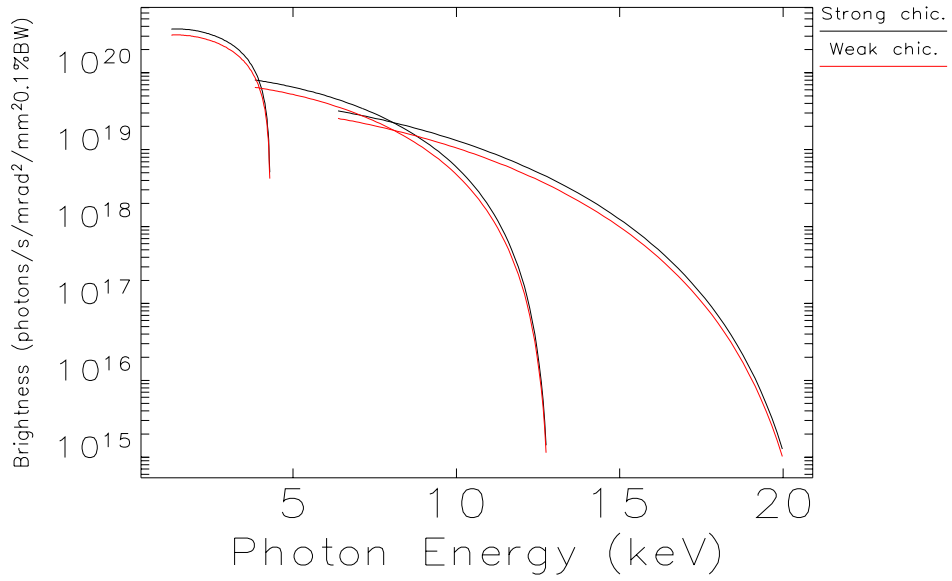


Figure 7: Peak brightness for a 2-nC, optimally compressed beam for the two chicane options, based on somewhat idealized initial tracking results.

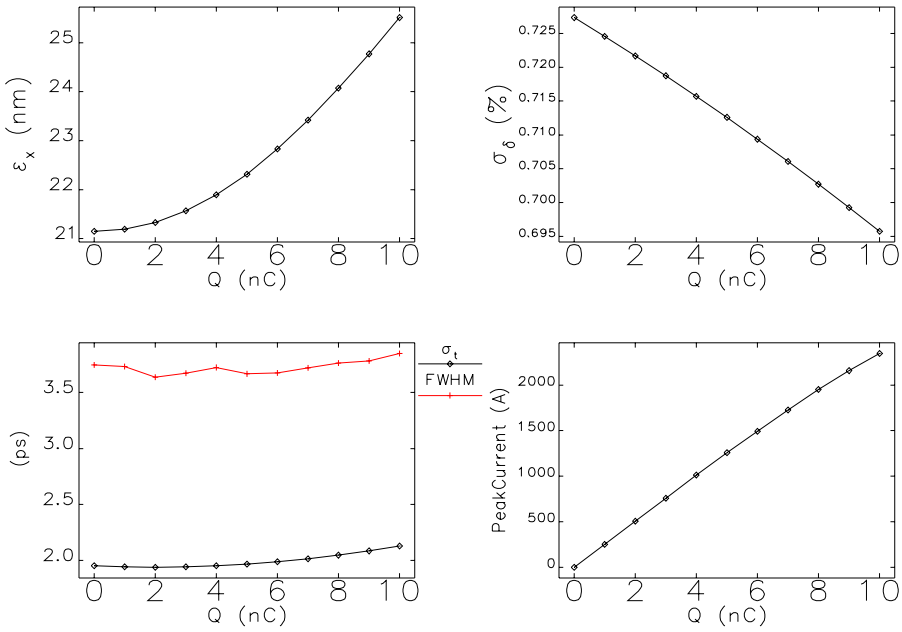


Figure 8: Beam properties at the end of the chicane as a function of charge including CSR and ISR.

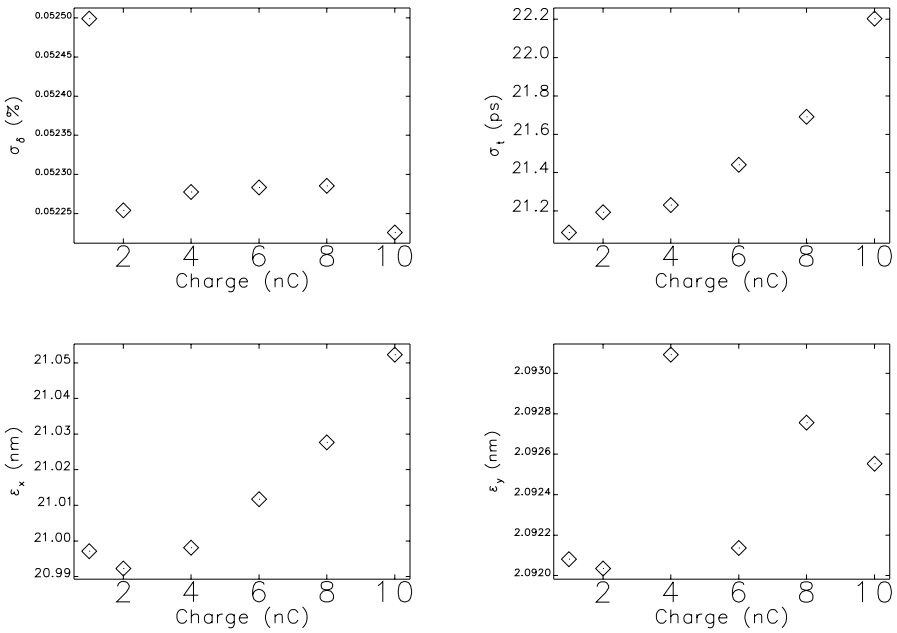


Figure 9: Beam properties from tracking to equilibrium in the booster.

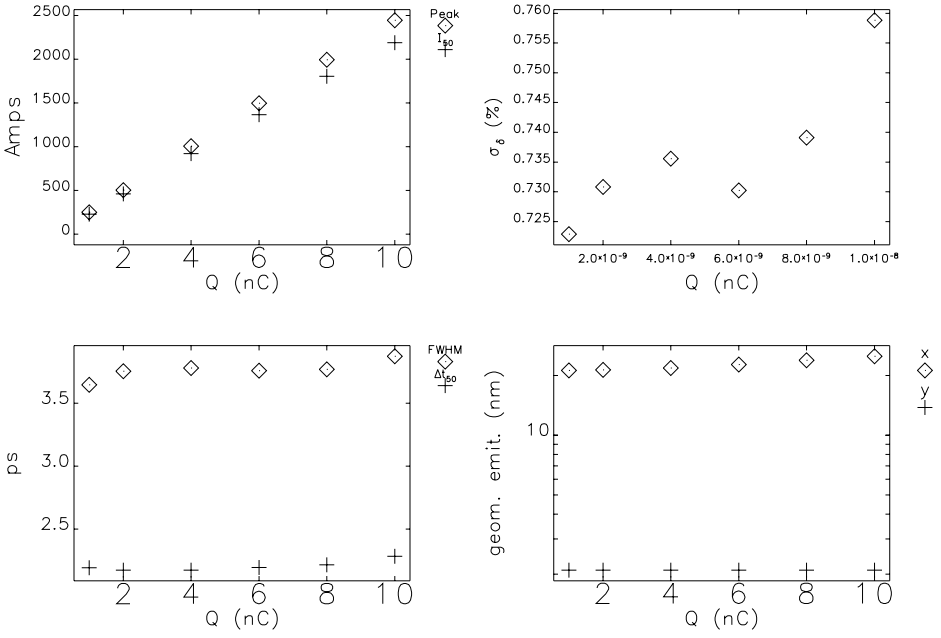


Figure 10: Results of tracking equilibrium booster beam through optimized compressors.

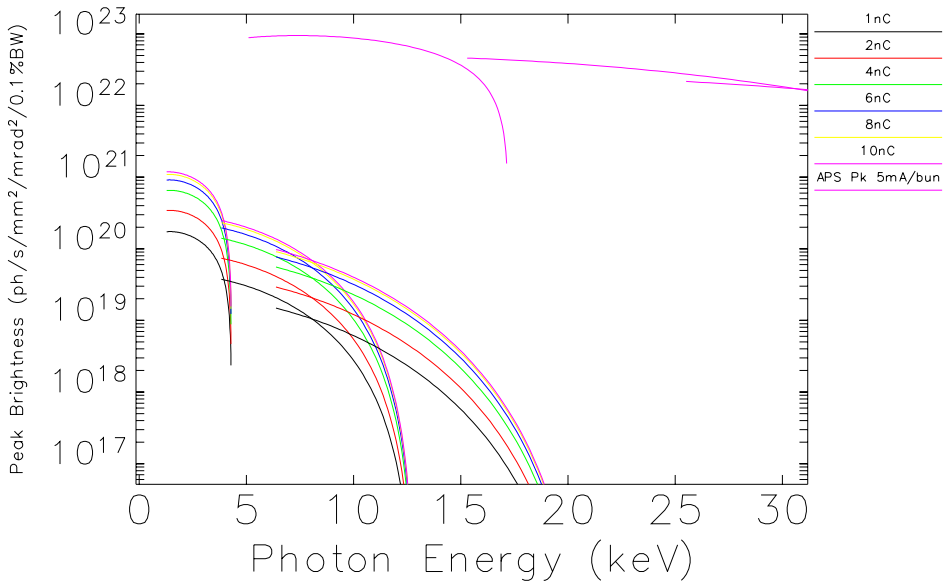


Figure 11: Peak brightness for U27 for the compressed booster beam and a typical 5-mA APS beam. The peak current for the booster beams is computed as $Q/(2\Delta t_{50})$, where $\Delta t_{50}$ is the duration of the central 50% of the beam. For the APS, the peak current is computed assuming a 5-mA Gaussian bunch of 10 mm rms length.

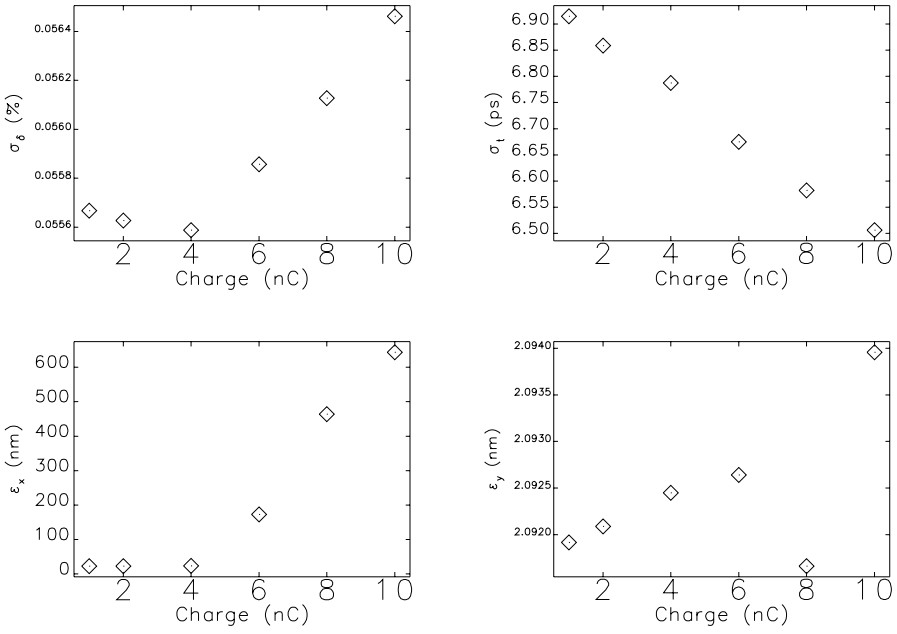


Figure 12: Beam properties from tracking to equilibrium in the booster with a $h = 3456$ higher-harmonic cavity.

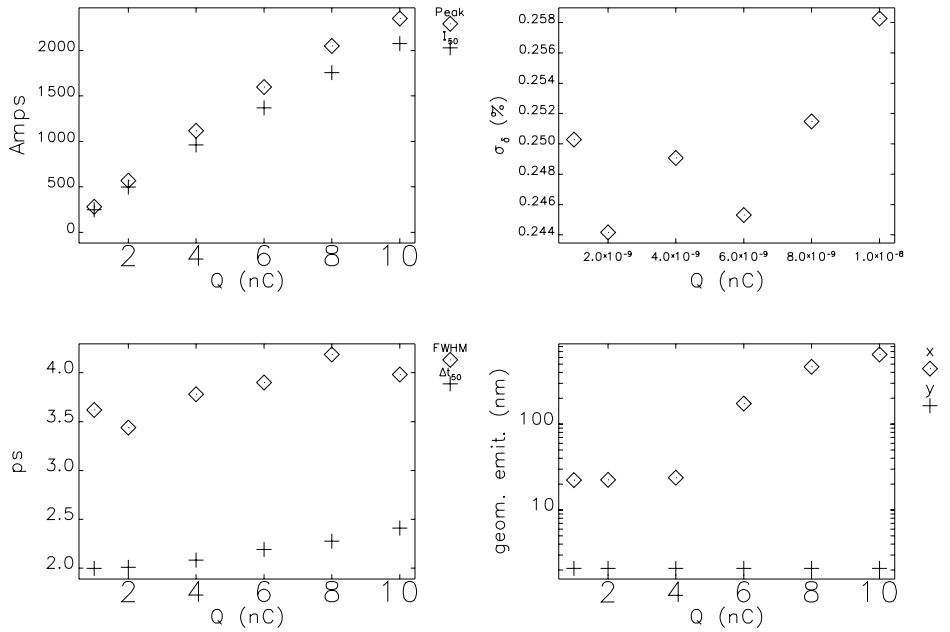


Figure 13: Results of tracking equilibrium booster beam with higher-harmonic cavity through optimized compressors.

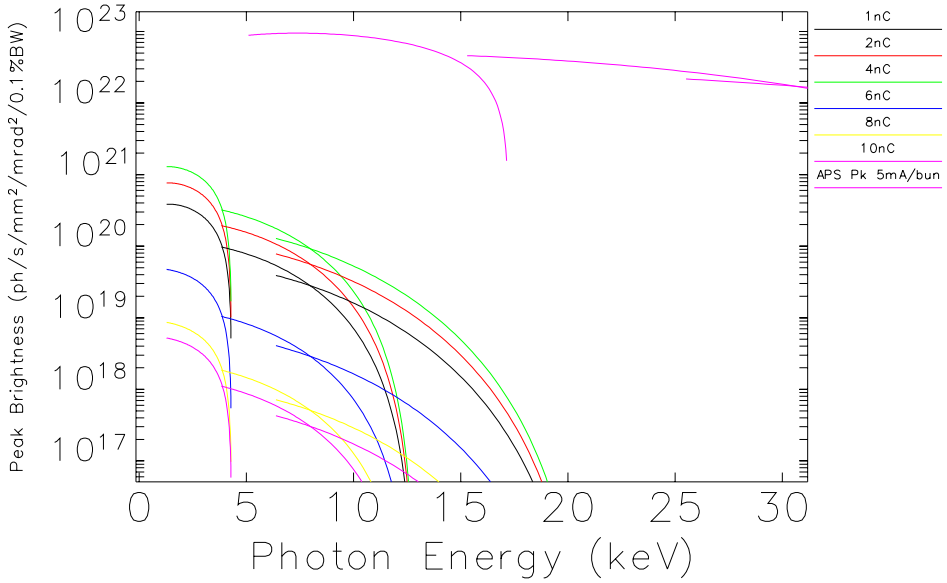


Figure 14: Peak brightness for U27 for the compressed booster beam with higher-harmonic cavity, along with results for a typical 5-mA APS beam. The peak current for the booster beams is computed as $Q/(2\Delta t_{50})$, where $\Delta t_{50}$ is the duration of the central 50% of the beam. For the APS, the peak current is computed assuming a 5-mA Gaussian bunch of 10 mm rms length.

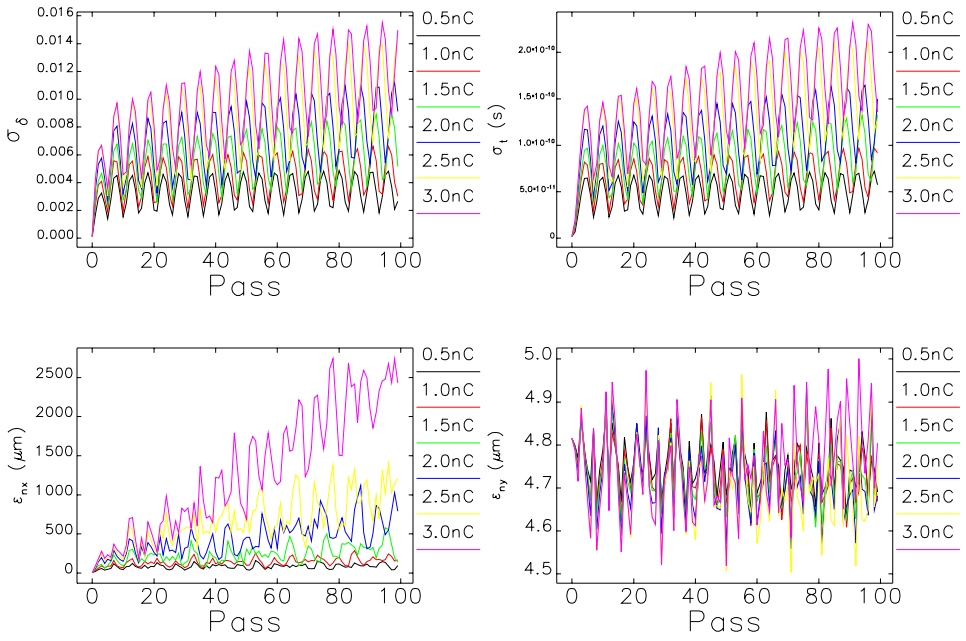


Figure 15: Results of tracking a photoinjector beam in the booster, including CSR effects.

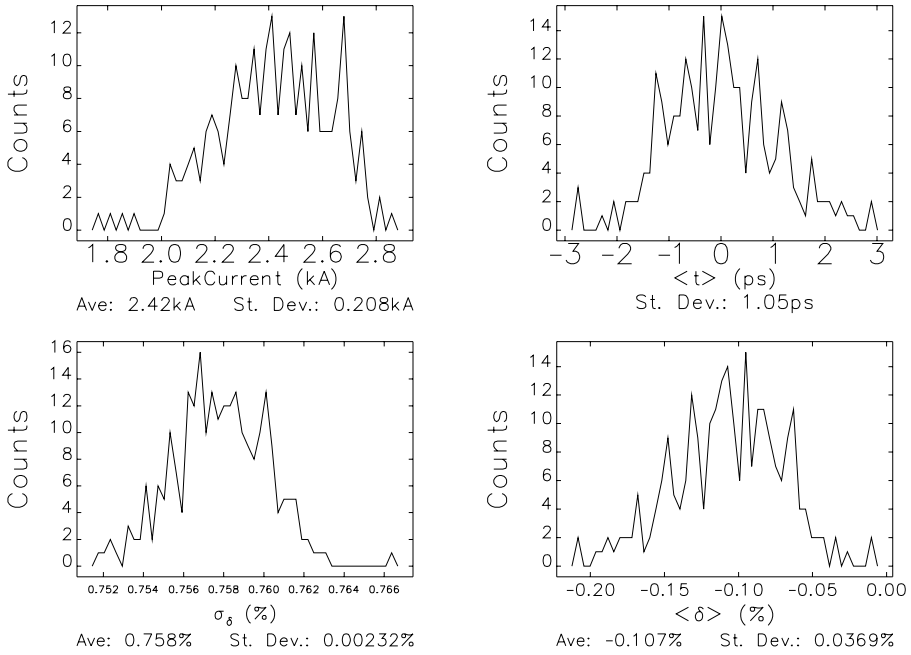


Figure 16: Histograms of selected beam properties in the presence of jitter .